International Journal of Approximate Reasoning 161 (2023) 108988

Contents lists available at ScienceDirect

International Journal of Approximate Reasoning

journal homepage: www.elsevier.com/locate/ijar

Physics-informed learning under epistemic uncertainty with an application to system health modeling

Luciano Sánchez *, Nahuel Costa, José Otero, Inés Couso

ARTICLE INFO

Article history:
Received 25 April 2023
Received in revised form 26 June 2023
Accepted 16 July 2023
Available online 22 July 2023

Keywords:
Remaining useful life
Physics-informed learning
Epistemic uncertainty
Maximum likelihood

ABSTRACT

This study proposes a methodology for developing deterioration models to estimate the remaining lifetime of a system using physics-informed learning. The approach consists of combining physical knowledge about the system with a set of data obtained from similar systems that have failed in the past to build a set of constraints on the evolution over time of the state of health of the system. The data consists of partial measurements of the system variables, taken from its commissioning to the present. The physical knowledge used comprises a set of differential equations that approximate the dynamics and aging of the system. In contrast to other studies, the physical model is not assumed to be accurate, but is considered to be an approximation of reality. Constraints on the temporal evolution of the state of health derived from this physical knowledge take into account its imprecision and consist of possibility distributions. In this study, the max-max, max-min and min-max regret principles are applied to extract the time evolution of the deterioration rate that best fits the constraints. The effectiveness of the proposed algorithm is evaluated by means of a comparative empirical analysis in different use cases, and the situations in which informed learning improves on purely data-driven algorithms are analyzed.

1. Introduction

Many physical systems deteriorate gradually over their lifetime, and sometimes events occur that cause failure or accelerate deterioration. These events can be caused by factors such as environmental changes, operating conditions, or wear and tear. Since failures are infrequent, assessing the current health of a system is often solved with anomaly detection techniques. Anomaly detection techniques involve identifying unusual patterns or behaviors in the system that may indicate a potential problem or failure.

In contrast, predicting the health of a system in the future involves extrapolating the current rate of deterioration to decide how long it will take for the equipment to degrade if the current operating conditions are maintained. In the literature, the first case is known as a condition monitoring (CM) problem, which involves monitoring the system for anomalies and identifying potential issues as they arise. The second case is known as a remaining useful life (RUL) estimation problem, which involves predicting how much longer the system can operate before it fails or requires maintenance.

Learning an anomaly detection system is usually based on data from systems that have operated until failure. In fact, it is not easy to measure the health status of systems that have not yet experienced a fault. The training set consists of various time series of measurements of the system's input and output variables from its commissioning to the end of its lifetime. The goal is to classify new series as either anomalous or normal. On the other hand, RUL models aim to predict, from the

* Corresponding author.
E-mail address: luciano@uniovi.es (L. Sánchez).

https://doi.org/10.1016/j.ijar.2023.108988

same training set, whether the system will reach premature end-of-life as far in advance as possible. RUL prediction is not a classification problem, but rather a problem of learning the lifetime probability distribution conditioned on the past values of the monitored system's variables.

In this paper, we present a methodology for Physics-Informed Learning (PIL) that enables the development of degradation models for forecasting the RUL of a system. PIL [11] is an approach that integrates physics-based knowledge as constraints in machine learning algorithms, i.e. instead of explicitly developing a mathematical model, PIL incorporates physical knowledge into the learning algorithm to improve accuracy and interpretability. In the present case, the learning problem consists of obtaining the time evolution of the state of health of a system from a partial set of measurements of the system variables. This work proposes to constrain the learning of a non-parametric degradation model with a set of soft bounds derived from the physical knowledge about the problem, intended to reduce the search space and guide learning towards the solutions of interest. The main contribution of this study consists in admitting that physical knowledge may be imprecise and cannot be transformed into a set of rigid constraints, but rather into the aforementioned set of soft constraints, which will be defined by possibility distributions. To solve the learning problem under this type of constraints, an implementation of the max-max, max-min and min-max regret principles [9] is proposed.

1.1. Literature review

RUL estimation streamlines inspection planning and establishes a maintenance policy that maximizes system performance across key criteria, including cost, availability, and reliability. In many cases, this estimation is based on stochastic deterioration models [24], as will be done in this study. Stochastic deterioration models can be grouped into three categories [1]: discrete-state and steady-state deterioration models, for environments where the system state is observable, and proportional hazard models for systems operating in dynamic environments [2]. Discrete-space methods are, in general, related to Markov processes [18] and steady-state methods are based on stochastic processes; in most cases, on Brownian motion [28], Gamma processes [14] or Gaussian and Inverse Gaussian [12].

The integration of stochastic methods and machine learning enables the development of more versatile predictive models, sometimes resulting in "black boxes" or fully data-driven approaches. These models are well-suited for scenarios where comprehensive data is available to capture all possible system operation and deterioration modes. However, in cases where data is incomplete, various methods exist to combine physical knowledge with data. One approach is the use of grey boxes or semi-physical models [15], which effectively integrate both types of knowledge, allowing for diagnostics in previously unseen scenarios and enhancing the interpretability of the deterioration model. Another approach, particularly in the field of failure prognosis, is PIL, which entails incorporating physical knowledge into black boxes by imposing constraints on the learning algorithm [10]. By introducing physical constraints into the machine learning models, PIL guides the search towards solutions that align with the underlying physics, reducing the need to explore a large number of candidate solutions [11].

Sources of uncertainty in PIL may be in the data (missing, noisy, censored data, etc.) as is the case with any other machine learning problem. However, in PIL, we are also interested in inaccuracies in prior physical knowledge because it is often a simplification of reality (unmodeled inputs, linearized equations, ignored effects, etc.) [25,31]. Since in PIL the learning is constrained to fit physical information about the system, the consequences of incorrect physical information can negate the benefits of the approach. This is an aspect that has only recently begun to be studied. In reference [19] it is mentioned that, in the context of PIL, the total uncertainty in function approximation depends on the usual factors: choice of parameters, hyperparameterization, optimization, sampling errors and also model misspecification, but then differentiates between uncertainties of a random nature in the data and of an epistemic nature in the a priori knowledge. The present work studies this second kind of uncertainty. We suggest that the representation of incomplete physical knowledge is related to previous research in epistemic, model-structure or model-form uncertainties [4,8]. In particular, in this study, we assume that the dynamic behavior and deterioration modes of the system under study are defined by a physics-informed loss function that incorporates physical principles represented by differential equations [29]. We also acknowledge that these differential equations provide a simplified representation of the physical processes involved, which may result in inconsistencies between the model and the data. Some authors have developed methods for selecting subsets of consistent data for inverse problems related to this [23]. We aim to identify the minimal-area region in the parameter space that can best explain the data (as done in [26] and other works). This involves generating a set of predictions by iterating through all the parameter values in this region and ensuring that this set covers the training data with a probability greater than or equal to a specified threshold. We repeat this process for different thresholds and assimilate the results into a possibility distribution over the parameter values [5,6]. Finally, we employ procedures similar to those developed for maximum likelihood inference from incomplete data [9] to obtain estimates of the system's health and remaining useful life from these set-valued models.

1.2. Novelty and contribution

New developments in this study are:

- Methodology for PIL of a RUL model from failed systems data and possibly inaccurate prior knowledge, where the physical constraints of the machine learning problem are expressed by means of possibility distributions.

- Particularization of the max-max, max-min and min-max regret strategies for handling soft constraints arising from epistemic uncertainty in physical knowledge.
- Comparative empirical study of the proposed algorithm, discussing the circumstances where informed learning improves purely data-driven algorithms.

1.3. Overview

The structure of this paper is as follows: Section 2 introduces the learning methodology and describes the uncertainty in the physics knowledge. Section 3 describes several case studies, including a problem related to the determination of the lifetime of a road tunnel fan and compares it with state-of-the-art methods in this field of application. The paper concludes in Section 4, where the conclusions of the study and future lines of research are presented.

2. Learning from precise data and imprecise expert knowledge

This section proposes a method for learning a RUL estimator for systems where only the initial (system without any deterioration) and final (system with known deterioration) States of Health (SoH) are known. It is also assumed that measurements of input and output variables are available and that there is physical knowledge of the system that can be exploited to select the most plausible SoH evolution between the two known states of health.

2.1. Stochastic deteriorations

The lifetime of a system is often assumed to be a stochastic process $\mathcal{L}(\tau)$, where τ can take on non-negative values. The expectation $E(\mathcal{L}(\tau))$ decreases as time progresses. The system's SoH is a value between 0 and 1, indicating the available fraction of the expected lifetime with respect to a newly commissioned system,

$$\mathrm{SoH}(\tau) = \frac{E(\mathcal{L}(\tau))}{E(\mathcal{L}(0))} \tag{1}$$

and the RUL of the system is defined as

$$\mathrm{RUL}(\tau) = E(\mathcal{L}(\tau)) = \mathrm{RUL}(0) \cdot \mathrm{SoH}(\tau). \tag{2}$$

The RUL learning problem is a statistical inference problem that consists in learning the parameters of the process $\mathcal{L}$ from a dataset comprising information measured over time on a sample of systems.

2.2. Possibilistic deteriorations and prior knowledge model

We denote time as τ, the inputs to the system as $\mathbf{u}$, the observed outputs as $\mathbf{y}$, the model predictions as $\hat{\mathbf{y}}$, and the (hidden) state variables as $\mathbf{x}$. The physical knowledge about the problem is given by the following three equations:

$$\dot{\mathbf{x}}(\tau) = f(\mathbf{x}(\tau), \mathbf{u}(\tau), \theta_f(\tau)) \tag{3}$$

$$\hat{\mathbf{y}}(\tau) = g(\mathbf{x}(\tau), \mathbf{u}(\tau), \theta_g(\tau)) \tag{4}$$

$$\widehat{\mathrm{SoH}}(\tau) = h(\theta_f(\tau), \theta_g(\tau)) \tag{5}$$

The evolution of the state and output variables over time is defined by the functions f and g, and the SoH of the system is defined by the function h. The parameters defining the functions f, g and h change over time to model the system's aging. We will assume that the expressions for f, g and h are known and that their parameters are fitted to the training data by the procedure discussed below.

Let the training set consist of a sequence of values of inputs and outputs of the system sampled at regular time intervals, $\tau = k\Delta t$, for $k = 1, \ldots, N$. Consider, to simplify the notation, that $\Delta t = 1$ and that the training set consists of pairs of input-output values of the system at these time instants,

$$(\mathbf{u}^*(0), \mathbf{y}^*(0)), (\mathbf{u}^*(1), \mathbf{y}^*(1)), \ldots, (\mathbf{u}^*(N), \mathbf{y}^*(N)). \tag{6}$$

The training set may also include data on the system's health. In this study, we are specifically interested in the case where the health is known to be 1 at the beginning of the sequence and 0 at the end. However, other cases can also be modeled, such as a complete set of health measures. For example, the system's health is often assumed to follow a piecewise linear profile, remaining constant until a point of deterioration and then linearly decreasing thereafter. In any case, let the training set also include the values of the system's health at certain time instants, denoted as T_{SoH}. Thus, the training data also contains $\{\mathrm{SoH}^*(t) : t \in T_{\mathrm{SoH}}\}$.

We will use the notation

$$\hat{\mathbf{y}}(\tau \mid \theta_f(\tau), \theta_g(\tau), \mathbf{x}_0) \tag{7}$$

to refer to the sequence of model outputs when the initial state is $\mathbf{x}_0$, the time evolution of the model parameters is $\theta_f(\tau)$, $\theta_g(\tau)$ and the inputs are a step function that takes the value $\mathbf{u}^*(t)$ for $t \leq \tau < t+1$.

Since equations (3), (4) and (5) are an approximation, it is in general not possible to find an initial state $\mathbf{x}(0)$ and parameter sequences $\theta_f^0(\tau)$ and $\theta_g^0(\tau)$ for which $\hat{\mathbf{y}}(t) = \mathbf{y}^*(t)$ at $t = 1, \ldots, N$ and $\widehat{\mathrm{SoH}}(t) = \mathrm{SoH}^*(t)$, for $t \in T_{\mathrm{SoH}}$, but we will assume that there is a time sequence of parameter sets $\Theta_f^0(\tau)$ and $\Theta_g^0(\tau)$ for which

$$\mathbf{y}^*(t) \in \{\hat{\mathbf{y}}(\tau \mid \theta_f(\tau), \theta_g(\tau), \mathbf{x}_0) : \theta_f(\tau) \in \Theta_f^0(\tau), \theta_g(\tau) \in \Theta_g^0(\tau)\} \tag{8}$$

and

$$\mathrm{SoH}^*(t) \in \{\widehat{\mathrm{SoH}}(\tau \mid \theta_f(\tau), \theta_g(\tau), \mathbf{x}_0) : \theta_f(\tau) \in \Theta_f^0(\tau), \theta_g(\tau) \in \Theta_g^0(\tau)\}. \tag{9}$$

In that case, we will be able to find a nested family of sets $\Theta_f^\alpha(\tau) \supseteq \Theta_f^\beta(\tau)$ for $\alpha \leq \beta$ (the definition of $\Theta_g^\alpha(\tau)$ is analogous) for which

$$Y^\alpha(\tau) = \{\hat{\mathbf{y}}(\tau \mid \theta_f(\tau), \theta_g(\tau), \mathbf{x}_0) : \theta_f(\tau) \in \Theta_f^\alpha(\tau), \theta_g(\tau) \in \Theta_g^\alpha(\tau)\} \tag{10}$$

$$S^\alpha(\tau) = \{\widehat{\mathrm{SoH}}(\tau \mid \theta_f(\tau), \theta_g(\tau), \mathbf{x}_0) : \theta_f(\tau) \in \Theta_f^\alpha(\tau), \theta_g(\tau) \in \Theta_g^\alpha(\tau)\} \tag{11}$$

$$|\{t : \mathbf{y}^*(t) \in Y^\alpha(t)), t = 1, \ldots, N\}| \geq (1-\alpha)N \tag{12}$$

$$|\{t : \mathrm{SoH}^*(t) \in S^\alpha(\tau)\}| \geq (1-\alpha)|(T_{\mathrm{SoH}})| \tag{13}$$

These nested families of parameters define two fuzzy sets $\widetilde{\mathbf{y}}(t)$ and $\widetilde{\mathrm{SoH}}(t)$, with membership functions

$$\widetilde{\mathbf{y}}(t, y) = \sup\{\alpha : y \in Y^\alpha(t)\} \tag{14}$$

$$\widetilde{\mathrm{SoH}}(t, s) = \sup\{\alpha : s \in S^\alpha(t)\} \tag{15}$$

that can be interpreted as conformal predictions of the approximate model of the system. This last fuzzy set will be interpreted as a possibility distribution Π_t that dominates the probability distribution P_t of $\widehat{\mathrm{SoH}}$ given t [5,6],

$$P_t(S) \leq \Pi_t(S) = \max_{s \in S} \widetilde{\mathrm{SoH}}(t, s). \tag{16}$$

Note that we are assuming that the set of possible health state values is discrete. Numerically fitting the parameters of the physical knowledge model consists of obtaining the nested sets of parameters $\Theta_f^\alpha(\tau)$ and $\Theta_g^\alpha(\tau)$ that are associated to the narrowest conformal predictions, that are the most specific fuzzy sets $\widetilde{\mathbf{y}}(t, y)$ and $\widetilde{\mathrm{SoH}}(t, s)$ that fulfill Eqs. (12) and (13). Section 3.1 develops an example illustrating these steps.

2.3. Degradation modes

We will suppose that a set C of different degradation modes is used and the model of the SoH is defined as the health of the most degraded mode by means of a set of functions h^c.

$$\widehat{\mathrm{SoH}}(\tau) = \min_{c \in C} \widehat{\mathrm{SoH}}^c(\tau) = \min_{c \in C} h^c(\theta_f(\tau), \theta_g(\tau)). \tag{17}$$

Expressing the SoH as the minimum of a collection of functions makes sense because silent degradations may appear in certain type of systems. These types of degradations are illustrated by the graphical example in Fig. 1. The system in this figure has two modes of deterioration. The first type of deterioration is noticeable at time $t = 4$, while the second type is initially masked by the first type and only becomes detectable at a later time. If the RUL prognosis of the system is based solely on the min SoH, the estimation would be overly optimistic until the second mode of deterioration appears. The correct estimation requires extrapolating both types of deteriorations and computing the minimum of the extrapolations. For this reason, this study will construct a health state estimator for each degradation mode in C and define the health of the system by combining all predictions.

2.4. Maximum likelihood estimation of the RUL

Given that the health of a system cannot improve on its own,

$$\mathrm{SoH}^c(\tau_1) \geq \mathrm{SoH}^c(\tau_2)\ \forall c \in C,\ \tau_2 \geq \tau_1 \tag{18}$$

we can assume that between two time instants $t-1$ and t, the SoH of the system under degradation mode c decreases by a factor $\delta^c(t) \in [0, 1]$:

$$\mathrm{SoH}^c(t) = \mathrm{SoH}^c(t-1) \cdot \delta^c(t) \tag{19}$$

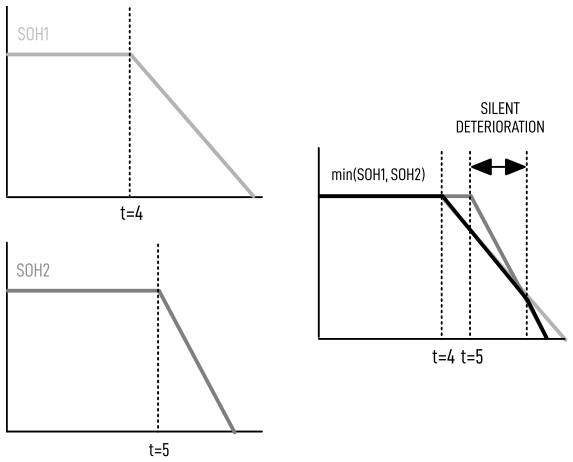

Fig. 1. Example of silent deterioration. Deterioration of the first type is noticeable at time $t = 4$, and deterioration of the second type would be noticeable at time $t = 5$, but is masked by the first and does not become detectable until later.

and

$$\mathrm{SoH}(t) = \min_{c \in C} \prod_{\tau=1}^{t} \delta^c(\tau). \tag{20}$$

Therefore, the RUL learning problem is equivalent to that of learning a matrix of deterioration speeds $[\delta^c(t)] \in \mathbf{D}$, with $\mathbf{D} = [0, 1]^{(\#C \times N)}$ comprising the values $\delta^c(t)$ for each time period t and each deterioration mode c.

Let the estimator of the deterioration rate of mode c of the system at time t be denoted by $\hat{\delta}^c(t)$. Choosing the values $\hat{\delta}^c(t)$ is equivalent to choosing a pair of parameters $\hat{\theta}_f(t)$ and $\hat{\theta}_g(t)$ such that (recall Eq. (17))

$$h^c(\hat{\theta}_f(t), \hat{\theta}_g(t)) = \prod_{\tau=1}^{t} \hat{\delta}^c(\tau). \tag{21}$$

The remaining part of this section discusses how to assign a likelihood to each possible D matrix, according to the soft constraints Π_t derived from the physical information about the system. As Eq. (16) indicates, the probability distribution of $\widehat{\mathrm{SoH}}(t)$ is dominated by Π_t. The likelihood function is not fully known, and various strategies can be employed to determine the best values of the parameters $\hat{\theta}_f(t)$ and $\hat{\theta}_g(t)$, which are discussed below.

Let $(\mathrm{SoH}(1), \ldots, \mathrm{SoH}(N))$ be a trajectory in the health state space encoded by the matrix D (recall Eq. (20)), and let P_t be the probability distribution of the system's health at time instant t. The probability of this trajectory is

$$P(D) = \prod_{t=1}^{N} P_t(\mathrm{SoH}(t)) \cdot \frac{1}{N} \tag{22}$$

where a uniform distribution of the time variable has been assumed. P_t is unknown, but it is dominated by Π_t, therefore

$$P(D) \in \mathbf{P}(D) = \left\{ \frac{1}{N^N} \prod_{t=1}^{N} p_t : p_t \in [0, \Pi_t(\mathrm{SoH}(t))] \right\} \tag{23}$$

In other words, given the way Π_t has been constructed, the likelihood of D (which is the logarithm of the probability of observing the training set, assuming the health evolution is given by D) is an element of the set

$$\mathbf{L}(D) = \left\{ \sum_{t=1}^{N} \log p_t : p_t \in [0, \Pi_t(\mathrm{SoH}(t))] \right\} \tag{24}$$

Note that we have disregarded the constant terms of the likelihood for the sake of notation simplification.

To choose the maximum likelihood trajectory, we propose three different strategies:

- Max-max strategy: This is an optimistic criterion. It assumes that $P_t(\mathrm{SoH}(t)) = \Pi_t(\mathrm{SoH}(t))$, so the likelihood function is

$$L_{\text{max-max}}(D) = \sum_{t=1}^{N} \log \Pi_t(\mathrm{SoH}), \tag{25}$$

and the best trajectory is

$$\widehat{D}_{\text{max-max}} = \arg\max_{D\in\mathbf{D}} L_{\text{max-max}}(D). \tag{26}$$

This solution seeks the trajectory in which the product of the membership values of the health state at each time instant is maximum, subject to the constraint that the values of $\text{SoH}(t)$ are decreasing.

- Max-min strategy: This is a pessimistic criterion. The values of $\mathbf{L}$ are restricted to the subset

$$\mathbf{L}_{\text{max-min}}(D) = \left\{ \sum_{t=1}^{N} \log p_t : p_t \in [\min_{q=1}^{N} \Pi_q(\text{SoH}(q)), \Pi_t(\text{SoH}(t))] \right\} \tag{27}$$

and the trajectory that maximizes the lower bound of $\mathbf{L}_{\text{max-min}}$ is chosen, where the likelihood is

$$L_{\text{max-min}}(D) = \sum_{t=1}^{N} \log \min_{q=1}^{N} \Pi_q(\text{SoH}(q)) = N \min_{q=1}^{N} \log \Pi_q(\text{SoH}(q)) \tag{28}$$

$$\widehat{D}_{\text{max-min}} = \arg\max_{D\in\mathbf{D}} L_{\text{max-min}}(D). \tag{29}$$

This solution seeks the sequence of SoH values for which the fulfillment of the constraint given by Π_t is, in the worst case, as good as possible.

- Min-max regret strategy: This is also a pessimistic strategy, defined based on a difference between likelihoods. Let the set $\mathbf{S}_t$ contain all feasible values of the SoH at time instant t (i.e. all values in $[0, 1]$ compatible with a monotonically decreasing system health), and let

$$\mathbf{R}_{\text{min-max}}(D) = \left\{ \sum_{t=1}^{N} (\log \max_{s\in\mathbf{S}_t} \Pi_t(s) - \log p_t) : p_t \in [0, \Pi_t(\text{SoH}(t))] \right\} \tag{30}$$

This difference is interpreted as the regret of not having chosen, at each time instant, the parameter value that is a priori the most likely. The trajectory that minimizes

$$R_{\text{min-max}}(D) = \sum_{t=1}^{N} (\log \max_{s\in\mathbf{S}_t} \Pi_t(s) - \log \Pi_t(\text{SoH})), \tag{31}$$

is chosen:

$$\widehat{D}_{\text{min-max-regret}} = \arg\min_{D\in\mathbf{D}} R_{\text{min-max}}(D). \tag{32}$$

3. Case studies

In this section, three use cases of the proposed methodology are studied. First, an illustrative example related to the diagnosis of the state of health of rechargeable lithium-ion batteries is explained in detail. Next, a road tunnel fan condition monitoring problem is developed. Finally, a comparative analysis is made between the proposed method and a selection of techniques based on the CMAPSS benchmark data [22].

3.1. State of health of li-ion batteries

First, all steps of the learning problem will be followed in a realistic battery diagnostic case. This problem is designed in such a way that it has a known solution and at the same time illustrates the usefulness of imprecise dynamical models for defining soft constraints for learning the RUL of a system.

Li-Ion batteries have charge zones where the voltage is highly dependent on the charge (especially when they are close to being fully charged or fully discharged) and others where the voltage is almost constant. Fig. 2 represents the voltage at the terminals of a hypothetical battery while charging at constant current, and the incremental capacity (IC) curve, which is the derivative of the charge with respect to the voltage.

In many cases, the behavior of a battery can be approximated by simple semi-physical analogies. Three such analogies are shown in Fig. 3. The left-hand side represents a mechanistic model, where the behavior of the battery is assimilated to that of a water tank. The volume of water in the tank is associated with the battery charge, and the height above ground is the battery terminal voltage. Observe that the tank is narrow at the ends and wide in the middle, and has the same shape as the IC curve. This model is accurate, but it can be difficult to adjust to partial charge cycles or when the charge current is high. A second semi-physical model, in this case an equivalent circuit model, is shown in the central part. It is assumed that the battery behaves as an RC circuit with a variable capacitor with a capacity profile also analogous to the IC curve [20]. This

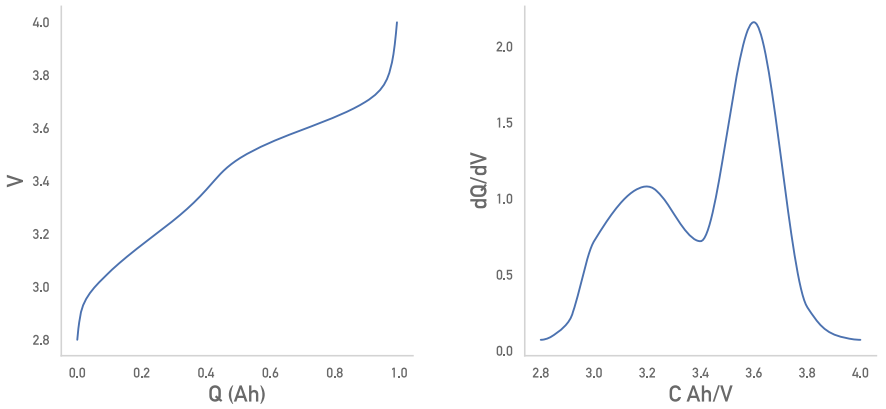

Fig. 2. Voltage at the terminals of a battery when charged at constant current. Left-hand side: when the battery is fully charged or discharged, the voltage variation with respect to the load is high. Right-hand side: Incremental capacity curve, or derivative of the charge with respect to the voltage.

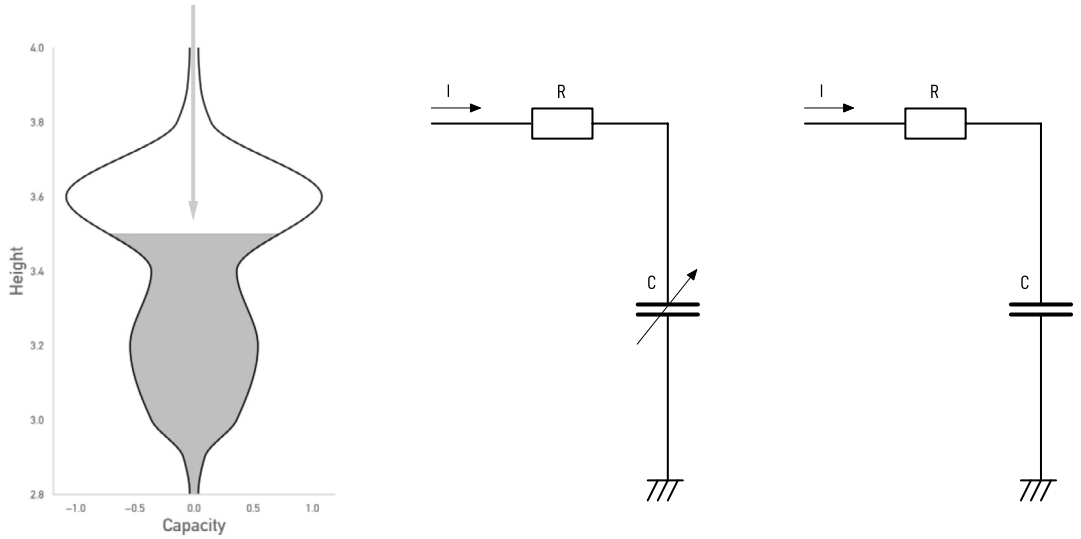

Fig. 3. Semi-physical models of a rechargeable li-ion battery. Left side: the water level in the tank is analogous to the battery voltage and the volume of water represents the charge stored in the battery. Middle part: variable capacitor model: the capacitance depends on the voltage, and this dependence is that of the diameter of the tank with respect to its height. Right side: Randles model: the capacitor has a constant capacity.

model is essentially the same as the one on the left, only with a different semi-physical analogy. The right-hand side shows the equivalent circuit model most commonly used in practice, the Randles model, where it is assumed that the capacity is constant (which is also equivalent to assuming that the tank is cylindrical). Randles' model is a rough approximation of reality (in addition, as this is a low frequency simulation, we have assumed that the charge transfer resistance is infinite to further simplify the circuit) and is not the best choice for a model-based PHM, but we will show that we can take advantage of it to define the constrains of a PIL problem.

The degradation of a battery depends on many factors. In this example, we will limit ourselves to only one deterioration mode: the increase in series resistance. In the mechanistic analogy, this resistance models the rate at which we can put water into the tank. This rate decreases as the battery degrades, or in other words, the resistance of the equivalent circuit model increases as the battery deteriorates.

In summary, in this example we will learn an physical-informed model of the State of Health (SoH) a battery, using the measured voltage data during a charge/discharge cycle, but we will not use an accurate model of the battery, as would be done in a conventional model-based diagnosis, but we will limit our physical knowledge of the problem to Randles' model, which as explained above implies a significant simplification of reality. For this we will generate data with the accurate (variable capacitor) model, increasing the series resistance with time, and then solve the PIL problem and study how close the max-max, max-min and min-max regret estimates are to the actual values of the series resistance.

The training data is the output of the simulated battery, that is computed by means of the following set of differential equations:

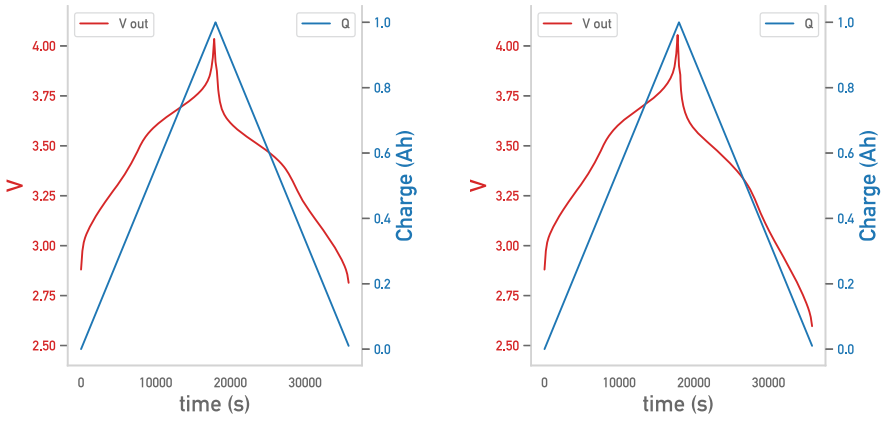

Fig. 4. Left-hand side: charge and discharge cycle of a non-degraded battery. Right side: charging and discharging cycle of a battery with progressive deterioration of the series resistance.

$$\dot{\mathbf{x}}(t) = C(\mathbf{x}(t))^{-1}\mathbf{u}(t) \tag{33}$$

$$\mathbf{y}(t) = \mathbf{x}(t) + uR(t) \tag{34}$$

where the state $\mathbf{x}$ is the voltage of the battery at rest, the input $\mathbf{u}$ is the charging current and the output $\mathbf{y}$ is the voltage. Fig. 4 shows the charge and voltage data of both a new battery and a deteriorated battery. Normal noise of mean 0 and standard deviation 0.1 was added to the training data. The capacity $C(\mathbf{x})$ depends on the battery terminal voltage as shown on the right-hand side of Fig. 2 (or, in the mechanistic analogy, C is the shape of the water tank and $\mathbf{x}$ is the height of the water in the tank). In this example we will assume that the true differential equations (33) and (34) are unknown and our knowledge is limited to Randles' approximate model:

$$\dot{\mathbf{x}}(t) = C^{-1}\mathbf{u}(t) \tag{35}$$

$$\mathbf{y}(t) = \mathbf{x}(t) + uR(t) \tag{36}$$

where C is constant (or, in the mechanistic analogy, the water tank is cylindrical). Expressing these equations in the notation used in this study,

$$\theta_f(t) = 1/C \tag{37}$$

$$\theta_g(t) = R \tag{38}$$

$$f(\mathbf{x}, \mathbf{u}, \theta_f(t)) = \theta_f(t) \cdot \mathbf{u}(t) \tag{39}$$

$$g(\mathbf{x}, \mathbf{u}, \theta_g(t)) = \mathbf{x} + \theta_g(t) \cdot \mathbf{u}(t) \tag{40}$$

$$h^1(\theta_f(t), \theta_g(t)) = \frac{1.5 - R(t)}{1.1} \tag{41}$$

where we have considered that the series resistance of an undeteriorated battery is 400 mΩ and that of a completely deteriorated battery is 1100 mΩ. In a real problem there would be more modes of deterioration and therefore there should be functions h^2, h^3, etc. that would depend on C, but in this example we stick to a single type of deterioration to simplify the explanation.

The next step is to search for the nested families Θ_f^α and Θ_g^α of parameter values. We look for a set-valued/conformal prediction $\{\hat{\mathbf{y}}(\theta_f, \theta_g) : \theta_f \in \Theta_f^\alpha, \theta_g \in \Theta_g^\alpha\}$ that covers the measured data measured with probability $1 - \alpha$. For simplicity, let us look for only one ϵ-cut and the modal point of this set, defined as follows:

$$\Theta_f^\epsilon = \Theta_f^1 = \{1/C\} \tag{42}$$

$$\Theta_g^\epsilon = [R^-(t), R^+(t)] \tag{43}$$

$$\Theta_g^1 = \{R^1(t)\} \tag{44}$$

which requires numerically determining values of C, $R^-(t)$, $R^+(t)$ and $R^1(t)$ for each time t in the training data (see Fig. 4). We want that the set of predictions has maximum specificity, subject to the fraction of non-covered points being less than ϵ. In this example, a sampling period of $\Delta t = 180$ s has been taken, and a linear dependence of R^- and R^+ with time was assumed. The best conformal prediction found is shown in Fig. 5.

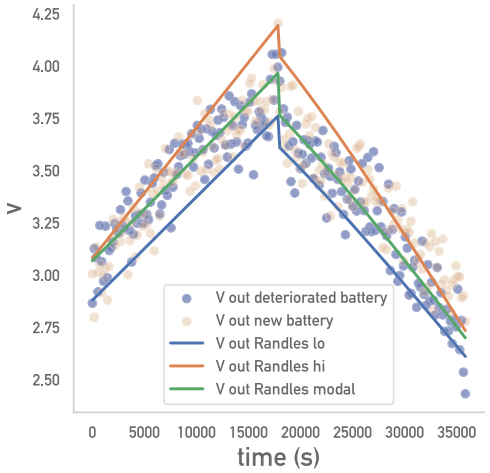

Fig. 5. Adjustment of the approximate physical model parameters (Randles' model with constant capacitor and interval-valued resistance). Note that the data has been contaminated with noise.

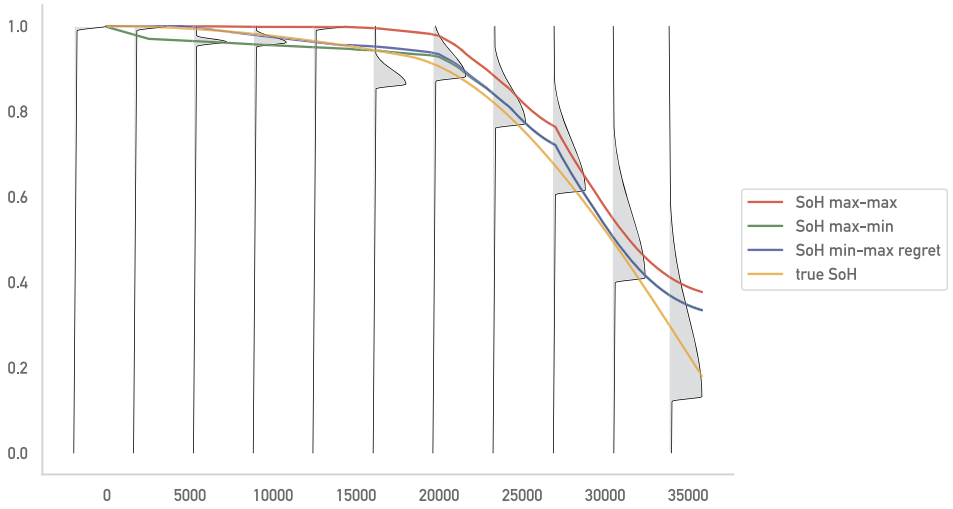

Fig. 6. Soft constraints on the health of the model (membership functions of the sets $\widetilde{\mathrm{SoH}}(\tau)$ for selected values of τ) and max-max, max-min and min-max regret estimates, compared to the actual SoH.

We then construct the soft constraints on the health of the model, i.e. the membership functions of the sets $\widetilde{\mathrm{SoH}}(\tau)$, whose α-cuts are the images of the sets Θ_f^α and Θ_g^α through h^1. We have assumed an asymmetric Gaussian membership for which the minimum of h^1 in Θ_g^ϵ is ϵ, as shown in Fig. 6. In this same figure the max-max, max-min and min-max regret estimates have been superimposed, together with the actual health state with which the data have been generated. The reconstruction is good despite the inaccuracy of Randles' mode, showing that the proposed approach is able to exploit useful information in imprecise physical knowledge.

3.2. Road tunnel fans

The left side of Fig. 7 depicts a 30 KW fan utilized for ventilation in road tunnels. These fans activate during hazardous conditions to protect occupants of vehicles traveling through the tunnel. Like all industrial machinery, gradual deterioration can occur and thus the equipment is periodically checked and monitored to detect any abnormal behavior. The fan's functioning can be influenced by several mechanical issues such as imbalances, insufficient lubrication, vibrations near the stall region, and unstable support. Electrical and electronic malfunctions, like electric motor or inverter failures may also impact the fan's operation.

Tests were conducted to know the dynamic behavior of the fan and its aging modes, deliberately inducing non-destructive failures such as removing lubricant from bearings or loosening brackets. The data gathered from these experiments were used to develop a differential equations-based model of the fan, that will be explained below.

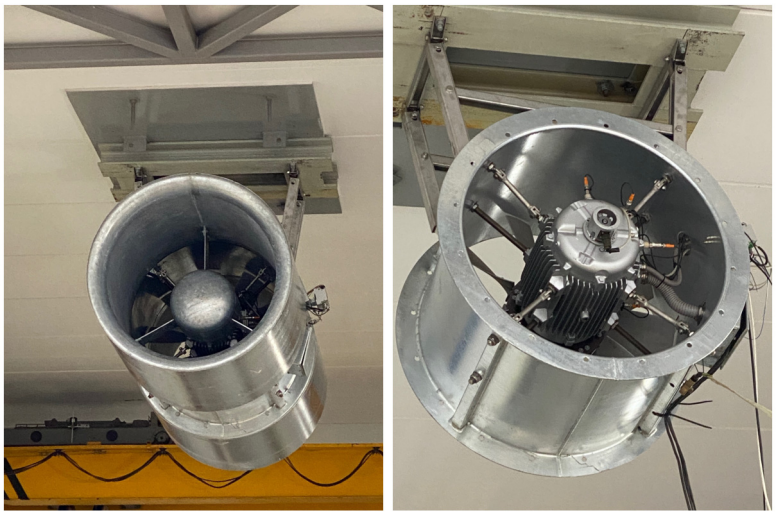

Fig. 7. 30 KW axial fan for road tunnel ventilation. Left side: fan with silencers. Right side: detail of the fan engine and the accelerometers used to measure vibrations.

3.3. Expert knowledge

The system is characterized by two inputs, namely, the rotational speed of the fan and the air flow rate, and eight outputs, which include temperatures in the three motor windings, temperatures in three bearings, and vibrations in two of the bearings. The outputs are not instantaneously dependent on the inputs, and the system model is defined by the following differential equations:

$$\dot{\mathbf{x}}(t) = \mathrm{A}\mathbf{x}(t) + \mathrm{B}\mathbf{u}(t) \tag{45}$$

$$\hat{\mathbf{y}}(t) = \mathrm{C}\mathbf{x}(t) + f_D(\mathbf{u}(t), [\mathrm{SoH}^1(t), \ldots, \mathrm{SoH}^8(t)]) \tag{46}$$

In this model, the matrices A, B, and C are invariant matrices that do not change over time and have dimensions $\mathbb{R}^{(1\times1)}$, $\mathbb{R}^{(1\times2)}$, and $\mathbb{R}^{(8\times1)}$, respectively. The nonlinear function $f_D(\cdot)$ determines the steady-state gains between the inputs and the outputs, and there are 24 parameters that affect this function, including a synthetic variable "pressure" with known cubic dependence on flow and velocity. In addition, there is linear dependence between the flow rate and pressure for winding temperatures, pressure and speed for bearing temperature, and flow rate and speed for vibrations. The parameters of $f_D(\mathbf{u}, [1, \ldots, 1])$ were measured with an undeteriorated fan, and those of $f_D(\mathbf{u}, [0, \ldots, 0])$ were measured with a fully deteriorated fan. We define $f_D(\mathbf{u}, .)$ as:

$$\begin{aligned} f_D(\mathbf{u}, [s^1, \ldots, s^8]) = \\ [s^1, \ldots, s^8] \cdot f_D(\mathbf{u}, [1, \ldots, 1]) + \\ [1 - s^1, \ldots, 1 - s^8] \cdot f_D(\mathbf{u}, [0, \ldots, 0]) \end{aligned} \tag{47}$$

A graphical representation of the model is shown in Fig. 8.

3.4. Compared statistical analysis

Four different validation sets have been generated, named 1P-1F, 4P-1F, 1P-4F, 4P-8F. The files include the eight output variables and the inputs (the operating point). The 1P-1F data set contains information measured at a single operating point (1P), and the fan suffers only one type of failure (1F), namely the front bearing. On the other hand, the 4P-8F dataset encompasses eight types of failure across four operating points. The datasets 1P-8F and 4P-1F are intermediate between the two. The training and test data files used in this analysis have been made publicly available at [27].

For the comparative analysis, the RVE method [3] has been applied to the four datasets. This method is representative of the state of the art in purely data-driven lifetime prediction in this type of problem. It is a generative neural network, specifically a variational autoencoder (VAE) trained on sequences of system outputs. The decoder in the VAE has been replaced by a regularized regression module that takes the latent variables of the autoencoder as inputs.

In Fig. 9, the left-hand side depicts the application of the RVE method to unit #7 in problem 1P-1F. The results show that the health estimate is not monotonic, but there is a noticeable decline in health at the time when deterioration occurs. The right-hand side of the same figure shows the results of the proposed method on the same fan. The max-max solution

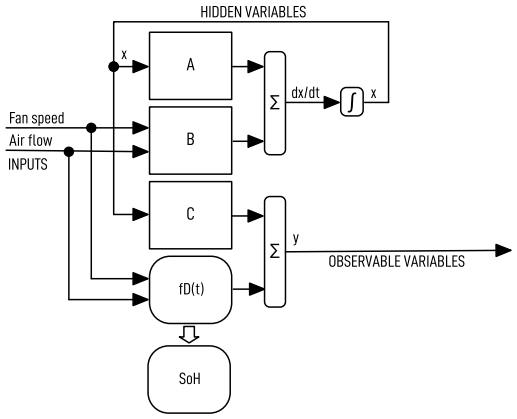

Fig. 8. Block diagram of the differential equations-based model of the fan.

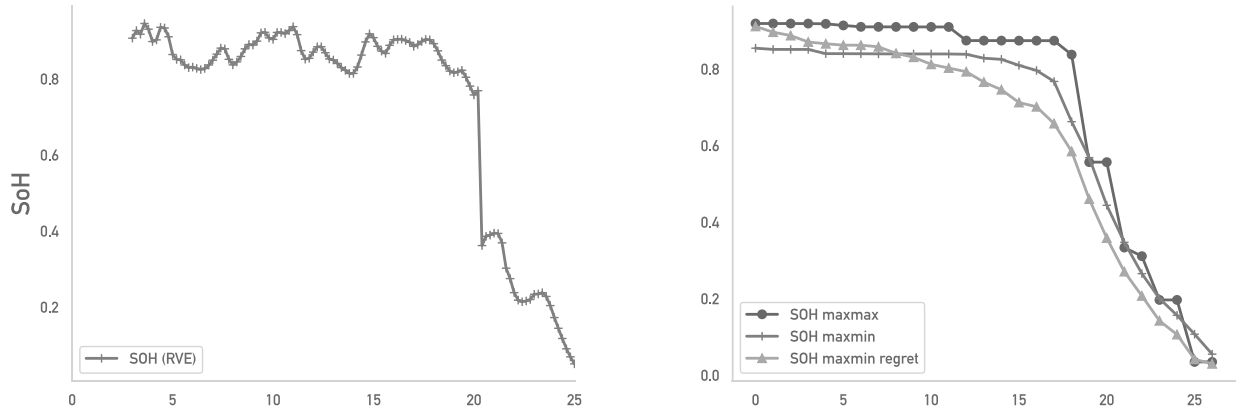

Fig. 9. Left-hand side: estimation of health status versus time in unit 7 of set 1P-1F using the RVE method, purely data-driven. Right hand side: min-min, min-max and min-max-regret estimates on the same ventilator, using informed physical learning.

Table 1
Mean absolute errors of RUL prediction, fan deterioration problems.

Method	1P-1F	4P-1F	1P-8F	4P-8F
Statistical (baseline)	66.12	55.97	46.62	48.95
RVE (state of the art)	35.48	37.29	30.31	**20.50**
Informed – Max-max Likelihood	21.70	23.93	20.80	24.13
Informed – Max-min Likelihood	**20.56**	23.39	**20.69**	23.28
Informed – Min-max Regret	20.76	**22.76**	20.70	23.69

produces the most optimistic estimate, while the max-min and min-max regret estimates are more conservative in their estimation. However, all three approaches correctly detect the evolution of health.

Finally, in Table 1 we present the mean absolute errors of the three methods presented in this study: estimations with imprecise informed models and particularizations of the max-max, max-min, and min-max-regret strategies discussed in the previous section. In this table we compare the results of informed learning with those of two purely data-driven methods, named “statistical” and the already mentioned “RVE”. The “statistical” method is currently used in industry and is based on the assumption that a conservative estimation of lifetime of a fan is known (i.e., the time between overhauls). The remaining lifetime is determined by deducting the effective operating time from the expected lifetime.

On average, physics-informed methods have been superior to alternative methods, performing better individually in three out of the four datasets studied. Due to a significant amount of noise in the measurements and the simplicity of the expert model, the max-min method, which selects the best model in the worst-case scenario, has proven to be the best alternative, followed by min-max-regret.

Although the volume of experimentation performed is not sufficient to draw strong conclusions, we observed that in problems 1P-1F and 4P-1F, informed methods are substantially better than methods purely guided by data, because the training sample does not cover all the situations of interest; the injected physical knowledge in the problem is compensating

for the lack of data. In 1P-8F and 4P-8F, the training data is more complete and therefore the results of data-driven methods improve. Informed learning methods may not achieve the same level of precision as data-driven methods because of the error inherent to the use of a simplified model; the use of strategies such as max-max, max-min, and min-max-regret improves the results compared to the uncorrected use of the physical model, but to match the RVE model applied to a complete set of training data, a more complex physical model would be required.

3.5. CMAPSS problem

To conclude the empirical study, a comparison will be made between different intelligent RUL prediction algorithms and this proposal on the CMAPSS benchmark [22]. Given that the objective of the algorithm presented in this paper is to make the most of the physical information available about the problem, this comparison will be carried out on a subset of this problem composed of a reduced number of variables, to which physical knowledge will be added.

Like the battery problem discussed in this section, the CMAPPS problem contains data from a simulator, in this case from a turbofan engine. Each of the four sets in this benchmark contains data on the evolution of different gas path variables of an aircraft engine, and the objective is to predict the number of cycles remaining until the health of the engine decreases below a threshold. In this problem, 20 variables are sampled at each operating cycle and, as will be seen below, some of the solutions in the state of the art are neural systems dependent on hundreds of thousands of parameters [3]. In this paper we will continue the line initiated in [21], aiming to develop a diagnostic system that balances accuracy with complexity.

To achieve this goal, we will use only two of the 20 system variables, in both cases related to the high-pressure compressor (HPC), which is the most failure-prone part in real data studies of this type of engine [16,17]. The variables chosen are "Pressure at Station 30" or P30, and "Temperature at Station 30", or T30. The adiabatic efficiency of the compressor can be approximated by a function of these variables and the temperature T0 and pressure P0 at the compressor inlet, as follows:

$$\eta = \frac{\left(\frac{\mathrm{P30}}{\mathrm{P0}}\right)^{\frac{\gamma-1}{\gamma}} - \mathrm{T0}}{\mathrm{T30} - \mathrm{T0}} \tag{48}$$

With a ratio of specific heats $\gamma \approx 1.4$. We will assume that there is a linear relationship between the RUL of the HPC and its efficiency,

$$\mathrm{SoH} = a\eta + b. \tag{49}$$

Adopting the notation introduced in this study, we define the variables

$$u = \mathrm{T30} \tag{50}$$

$$y = \mathrm{P30} \tag{51}$$

and the following equations:

$$\dot{x} = \theta_1 x + u \tag{52}$$

$$y = \theta_4(\theta_2 + \theta_3(t)(x - \theta_2))^{3.5} \tag{53}$$

The state variable x is a smoothing of T30, intended to reduce the noise in this signal. The parameter $\theta_3(t)$ is the adiabatic efficiency of the compressor, and the parameters θ_2 and θ_4 model T0 and P0 respectively. Therefore,

$$\theta_f(t) = \theta_1 \tag{54}$$

$$\theta_g(t) = (\theta_2, \theta_3(t), \theta_4) \tag{55}$$

$$f(\mathbf{x}, \mathbf{u}, \theta_f(t)) = \theta_1 x + u \tag{56}$$

$$g(\mathbf{x}, \mathbf{u}, \theta_f(t)) = \theta_4(\theta_2 + \theta_3(t)(x - \theta_2))^{3.5} \tag{57}$$

$$h^1(\theta_f(t), \theta_g(t)) = a \cdot \theta_3(t) + b \tag{58}$$

In order to determine the sets Θ_f^α and Θ_g^α we consider that the SoH of each engine decreases linearly from 1 to 0 in the last 125 cycles of each trajectory. The parameter $\theta_3(t)$ is also considered to be monotonically decreasing in time.

The results are shown in Table 2. The upper part of the table contains the state of the art in RUL prediction for the CMAPPS problem. The most accurate algorithms, such as MS-DCNN [13] or RVE [3] are large neural networks. Recent algorithms, such as SAM [21] depend on a reduced number of parameters, as is the case of the algorithm introduced in this study. Note that, despite being based on only two variables and six parameters, the introduction of an approximate physical knowledge (the adiabatic efficiency of a compressor under ideal conditions) leads, according to the metric proposed by the benchmark authors, to the best alternative in the two problems (FD002 and FD004) where the engine operates at several different operating points.

Table 2
Comparison of results on a selection of intelligent techniques applied to the CMAPSS problem (upper part of the table reproduced from reference [21]).

	FD001		FD002		FD003		FD004	
	RMSE	Score	RMSE	Score	RMSE	Score	RMSE	Score
MLP [30]	37.56	18000	80.03	7800000	37.39	17400	77.37	5620000
SVR [30]	20.96	1380	42.00	590000	21.05	1600	45.35	371000
RVR [30]	23.80	1500	31.30	17400	22.37	1430	34.34	26500
CNN [30]	18.45	1299	30.29	13600	19.82	1600	29.16	7890
Deep LSTM [30]	16.14	338	24.49	4450	16.18	852	28.17	5550
Semi-Supervised [7]	12.56	231	22.73	3366	12.10	251	22.66	2840
DCNN [13]	12.61	273	22.36	10412	12.64	284	23.31	12466
MS-DCNN [13]	**11.44**	**196**	19.35	3747	**11.67**	**241**	22.22	4844
VAE+RNN [3]	15.81	326	24.12	4183	14.88	722	26.54	5634
RVE [3]	13.42	323	**14.92**	1379	12.51	256	**16.37**	1846
SAM [21]	16.79	437	19.51	1555	17.48	588	22.82	3960
PIL max-max	20.69	535	22.81	1721	17.12	407	18.70	**1711**
PIL max-min	15.74	328	17.36	**1058**	16.99	478	18.90	1984
PIL min-max regret	15.11	315	17.36	1059	16.99	478	18.90	1984

4. Concluding remarks and future work

The study concludes that models incorporating prior physical information are advantageous in situations where available datasets are incomplete, and additional knowledge is necessary to generalize to unknown scenarios. It has been shown that, even if the physical information is incomplete, it can be used to construct a set of constraints to the SoH learning problem that guide learning towards the solutions of interest. Unlike previous work in model-based PHM, where the system model is assumed to be correct, or in PIL, where physical knowledge about the problem is translated into hard constraints, in this study physical knowledge is not assumed to be accurate, and is therefore transformed into soft constraints, which must be met only to a certain extent. The max-max, max-min and min-max-regret strategies define how estimates of the health of the system may or may not meet the set of constraints.

From a conceptual standpoint, we combined a precise training set and approximate differential equations to construct a possibility distribution that bounds the probability distribution of the health model at each moment in time. This possibility distribution was then combined with constraints on the evolution of the state of health over time, and we particularized three strategies (min-min, min-max, min-max-regret) to produce a precise estimate of the system's health at each time instant. Our procedure to construct the possibility distribution was based on the interpretation of a possibility as a nested family of confidence intervals, but other alternatives exist. Specifically, we believe it is possible to construct the set of maximum-likelihood estimates of the model parameters for different subsets of the training set and assign probabilities to these estimates based on the goodness of fit and the cardinality of each subset. We will explore these alternatives in future work.

Declaration of competing interest

The authors declare that they have no known competing financial interests or personal relationships that could have appeared to influence the work reported in this paper.

Data availability

Data has been made publicly available at Mendeley Data.

Acknowledgements

Supported by Ministerio de Economía e Industria de España, grant PID2020-112726RB-I00 and by Principado de Asturias, grant SV-PA-21-AYUD/2021/50994.

References

[1] Suzan Alaswad, Yisha Xiang, A review on condition-based maintenance optimization models for stochastically deteriorating system, Reliab. Eng. Syst. Saf. 157 (2017) 54–63.
[2] Kamyar Azar, Zohreh Hajiakhondi-Meybodi, Farnoosh Naderkhani, Semi-supervised clustering-based method for fault diagnosis and prognosis: a case study, Reliab. Eng. Syst. Saf. 222 (2022) 108405.
[3] Nahuel Costa, Luciano Sánchez, Variational encoding approach for interpretable assessment of remaining useful life estimation, Reliab. Eng. Syst. Saf. 222 (2022) 108353.
[4] Inés Couso, Didier Dubois, Statistical reasoning with set-valued information: ontic vs. epistemic views, Int. J. Approx. Reason. 55 (7) (2014) 1502–1518.

[5] Inés Couso, Susana Montes, Pedro Gil, The necessity of the strong α-cuts of a fuzzy set, Int. J. Uncertain. Fuzziness Knowl.-Based Syst. 9 (02) (2001) 249–262.
[6] Didier Dubois, Laurent Foulloy, Gilles Mauris, Henri Prade, Probability-possibility transformations, triangular fuzzy sets, and probabilistic inequalities, Reliab. Comput. 10 (4) (2004) 273–297.
[7] André Listou Ellefsen, Emil Bjørlykhaug, Vilmar Æsøy, Sergey Ushakov, Houxiang Zhang, Remaining useful life predictions for turbofan engine degradation using semi-supervised deep architecture, Reliab. Eng. Syst. Saf. 183 (2019) 240–251.
[8] Scott Ferson, Model uncertainty in risk analysis, in: Proc. 6th International Workshop on Reliable Engineering Computing, REC2014, Illinois, USA, 2014, pp. 27–43.
[9] Romain Guillaume, Didier Dubois, A min-max regret approach to maximum likelihood inference under incomplete data, Int. J. Approx. Reason. 121 (2020) 135–149.
[10] Chao Hu, Kai Goebel, David Howey, Zhike Peng, Dong Wang, Peng Wang, Byeng D. Youn, Special issue on physics-informed machine learning enabling fault feature extraction and robust failure prognosis, Mech. Syst. Signal Process. 192 (2023) 110219.
[11] George Em Karniadakis, Ioannis G. Kevrekidis, Lu Lu, Paris Perdikaris, Sifan Wang, Liu Yang, Physics-informed machine learning, Nat. Rev. Phys. 3 (6) (2021) 422–440.
[12] Juseong Lee, Mihaela Mitici, Multi-objective design of aircraft maintenance using Gaussian process learning and adaptive sampling, Reliab. Eng. Syst. Saf. 218 (2022) 108123.
[13] Han Li, Wei Zhao, Yuxi Zhang, Enrico Zio, Remaining useful life prediction using multi-scale deep convolutional neural network, Appl. Soft Comput. 89 (2020) 106113.
[14] Xingheng Liu, José Matias, Johannes Jäschke, Jørn Vatn, Gibbs sampler for noisy transformed gamma process: inference and remaining useful life estimation, Reliab. Eng. Syst. Saf. 217 (2022) 108084.
[15] Ljung Lennart, Perspectives on system identification, Annu. Rev. Control 34 (1) (2010) 1–12.
[16] Alvaro Martínez, Luciano Sánchez, Inés Couso, Engine health monitoring for engine fleets using fuzzy radviz, in: 2013 IEEE International Conference on Fuzzy Systems (FUZZ-IEEE), IEEE, 2013, pp. 1–8.
[17] Alvaro Martínez, Luciano Sánchez, Inés Couso, Aeroengine prognosis through genetic distal learning applied to uncertain engine health monitoring data, in: 2014 IEEE International Conference on Fuzzy Systems (FUZZ-IEEE), IEEE, 2014, pp. 1945–1952.
[18] Van-Thai Nguyen, Phuc Do, Alexandre Vosin, Benoit Iung, Artificial-intelligence-based maintenance decision-making and optimization for multi-state component systems, Reliab. Eng. Syst. Saf. 228 (2022) 108757.
[19] Apostolos F. Psaros, Xuhui Meng, Zongren Zou, Ling Guo, George Em Karniadakis, Uncertainty quantification in scientific machine learning: methods, metrics, and comparisons, J. Comput. Phys. (2023) 111902.
[20] Luciano Sanchez, Cecilio Blanco, Juan C. Anton, Victor Garcia, Manuela Gonzalez, Juan C. Viera, A variable effective capacity model for LiFePO4 traction batteries using computational intelligence techniques, IEEE Trans. Ind. Electron. 62 (1) (2014) 555–563.
[21] Luciano Sánchez, Nahuel Costa, Inés Couso, Simplified models of remaining useful life based on stochastic orderings, Reliab. Eng. Syst. Saf. 237 (2023) 109321.
[22] Abhinav Saxena, Kai Goebel, Don Simon, Neil Eklund, Damage propagation modeling for aircraft engine run-to-failure simulation, in: 2008 International Conference on Prognostics and Health Management, IEEE, 2008, pp. 1–9.
[23] Krushna Shinde, Pierre Feissel, Sébastien Destercke, Dealing with inconsistent measurements in inverse problems: set-based approach, Int. J. Uncertain. Quantificat. 11 (3) (2021).
[24] Xiao-Sheng Si, Wenbin Wang, Chang-Hua Hu, Dong-Hua Zhou, Remaining useful life estimation—a review on the statistical data driven approaches, Eur. J. Oper. Res. 213 (1) (2011) 1–14.
[25] Michail Spitieris, Ingelin Steinsland, Bayesian calibration of imperfect computer models using physics-informed priors, J. Mach. Learn. Res. 24 (108) (2023) 1–39.
[26] Liqi Sui, Pierre Feissel, Thierry Denoeux, Identification of elastic properties in the belief function framework, Int. J. Approx. Reason. 101 (2018) 69–87.
[27] Luciano Sánchez, Nahuel Costa, Inés Couso, Condition monitoring of axial fans for road tunnels, Mendeley Data V1 (2023), https://doi.org/10.17632/mzjvw6kbt7.1.
[28] Yukun Wang, Xiaopeng Li, Junyan Chen, Yiliu Liu, A condition-based maintenance policy for multi-component systems subject to stochastic and economic dependencies, Reliab. Eng. Syst. Saf. 219 (2022) 108174.
[29] Yanwen Xu, Sara Kohtz, Jessica Boakye, Paolo Gardoni, Pingfeng Wang, Physics-informed machine learning for reliability and systems safety applications: state of the art and challenges, Reliab. Eng. Syst. Saf. 230 (2023) 108900.
[30] Shuai Zheng, Kosta Ristovski, Ahmed Farahat, Chetan Gupta, Long short-term memory network for remaining useful life estimation, in: 2017 IEEE International Conference on Prognostics and Health Management (ICPHM), IEEE, 2017, pp. 88–95.
[31] Yingzhe Zheng, Zhe Wu, Physics-informed online machine learning and predictive control of nonlinear processes with parameter uncertainty, Ind. Eng. Chem. Res. 62 (6) (2023) 2804–2818.